Journal of Solid State Chemistry 192 (2012) 81–86

Contents lists available at SciVerse ScienceDirect

Journal of Solid State Chemistry

journal homepage: www.elsevier.com/locate/jssc

Synthesis, structure, and electrical resistivity of $Cs_3U_{18}Se_{38}$

George N. Oh, James A. Ibers *

Department of Chemistry, Northwestern University, 2145 Sheridan Road, Evanston, IL 60208-3113, USA

ARTICLE INFO

Article history:
Received 24 October 2011
Received in revised form
9 February 2012
Accepted 12 February 2012
Available online 29 March 2012

Keywords:
Cesium uranium selenide
Single-crystal X-ray structure
Charge balance
Single-crystal electrical resistivity

ABSTRACT

$Cs_3U_{18}Se_{38}$ was synthesized by the solid-state reactions of U, Se, CsCl or Cs_2Se_3, and P or As at 1273 K. This compound crystallizes in a new structure in the tetragonal space group D_{4h}^{18}-*I*4/*mcm*. The asymmetric unit contains U atoms in four different coordination environments. The overall three-dimensional network structure contains channels along the *c* axis, in which the Cs atoms lie. The formula $Cs_3U_{18}Se_{38}$ does not charge balance with the typical formal oxidation states of the elements. Electrical resistivity measurements conducted on a single crystal reveal a broad feature at 225 K, atypical semiconductor behavior below 57 K, and a calculated band gap of 0.0030(1) eV.

1. Introduction

Investigations of the ternary systems containing an alkali metal, uranium, and a chalcogen (A=Li–Cs; Q=S, Se, Te) have found compounds that crystallize in only a few structure types. Compounds containing lighter alkali metals, including Li_2US_3 and Na_2US_3, crystallize in the monoclinic space group *C*2/*m*, isostructural with compounds $ALnS_2$ (Ln=lanthanide) [1]. K_2UTe_3 and Rb_2UTe_3 are also isostructural with $ALnS_2$ [2]. In these compounds, uranium, which is octahedrally coordinated by six Q atoms, is tetravalent and there is no Q–Q bonding. KUS_2 crystallizes in the tetragonal space group *P*4/*nmm*, and the absence of Q–Q bonding suggests that the uranium is trivalent. This is supported by magnetic measurements [3]. In contrast, compounds with formulas AU_2Q_6 generally contain some degree of Q–Q bonding [4]. The majority of compounds in the A/U/Q system have this formula. Other actinides crystallize in these structure types as well [4,5]. AAn_2Q_6 compounds crystallize in one of two structure types. AU_2Se_6 (A=K, Rb, Cs) [4,6,7] crystallize in the KTh_2Se_6 [8] structure type, in the orthorhombic space group *Immm*, as do $RbTh_2Se_6$ [8], KNp_2Se_6, and $CsNp_2Se_6$ [4]. $CsTh_2Te_6$ crystallizes in a closely related structure [9] of the orthorhombic space group *Cmcm*, as does KTh_2Te_6 [5]. Physical measurements suggest tetravalent uranium for these uranium compounds, but assigning such an oxidation state fails to achieve charge balance. The difficulties in assigning these oxidation states have been discussed in detail [4].

$CsUTe_6$ crystallizes in an unrelated chain structure and contains U in a tricapped-trigonal-prismatic coordination environment [10]. Another A/U/Q compound is K_4USe_8, which crystallizes in the orthorhombic space group *Fdd*2 [11]. This compound contains discrete $[U(Se_2)_4]^{4-}$ anions where the U atom is coordinated by Se in a triangulated dodecahedral arrangement.

Here we report the synthesis, structure, and electrical resistivity of $Cs_3U_{18}Se_{38}$, a new compound that contains an alkali metal, uranium, and a chalcogen.

2. Experimental

2.1. Syntheses

U filings (Oak Ridge National Laboratory) were powdered by hydridization and subsequent decomposition under heat and vacuum [12], in a modification of a previous literature method [13]. UP_2 was synthesized by the stoichiometric reaction of U and red P (Aldrich, 99.9%) at 1273 K in a sealed fused-silica tube. Cs_2Se_3 was synthesized by the stoichiometric reaction of Cs (Aldrich, 99.5%) and Se (Cerac, 99.999%) in liquid ammonia at 194 K [14]. CsCl (Aldrich, 99.9%), Ni (Alfa, m3N), and As (Strem, 2N) were used as obtained.

$Cs_3U_{18}Se_{38}$ was synthesized in the highest yields in the reaction of UP_2 (0.10 mmol), Ni (0.05 mmol), Se (0.20 mmol), and CsCl (1.20 mmol). The reagents were loaded into a 6 mm-diameter carbon-coated fused-silica tube in an argon-filled glove box; the tube was then removed and flame-sealed under 10^{-4} Torr vacuum. The tube was placed in a computer-controlled furnace and heated to 1273 K in 96 h, held there for 4 h, cooled to 1223 K in 12 h, held there for 96 h, cooled to 1073 K in 12 h, held there for 96 h, then cooled to 298 K in 192 h. Washing the

* Corresponding author. Fax: +1 18474912976.
E-mail address: ibers@chem.northwestern.edu (J.A. Ibers).

0022-4596/$ - see front matter © 2012 Elsevier Inc. All rights reserved.
http://dx.doi.org/10.1016/j.jssc.2012.02.035

contents in water afforded black irregularly shaped blocks of $Cs_3U_{18}Se_{38}$ in roughly 5 wt% yield, based on U. Qualitative EDS analysis with a Hitachi-S3400 SEM on single crystals identified the presence of significant amounts of Cs, U, and Se, and no P, Cl, or Ni. A prism-shaped crystal with longest dimension 230 μm was selected for the crystal-structure determination.

$Cs_3U_{18}Se_{38}$ was also synthesized by the reaction of U (0.126 mmol), Se (0.214 mmol), Cs_2Se_3 (0.013 mmol), and As (0.063 mmol), with the same heating profile. The ten crystals found in this reaction were well-formed and highly faceted, though much smaller, 10 μm or less along the longest dimension. The identical reaction without As afforded only three crystals. One of the crystals from the As-assisted reaction was used for a second crystal-structure determination. One large crystal in the shape of a rod with tapered tips was selected for single-crystal resistivity measurements.

In all of these reactions, the primary products were flat black needles of CsU_2Se_6 [7] and β-USe_2 [15]. Estimated amounts of CsU_2Se_6 and β-USe_2 were 60 to 70 wt% and 20 wt%, respectively. $Cs_3U_{18}Se_{38}$ is sparingly soluble in 5% NaOH. It partly decomposes into a red powder in 5% HNO_3, also evolving a few bubbles, indicative of H_2Se formation.

2.2. Structure determination

Full spheres of data were collected on a Bruker APEXII platform diffractometer. The data consisted of ω scans at $\phi=0^\circ$, 90°, 180°, and 270°, taken at a detector distance of 60 mm. Each scan consisted of 606 frames. Frames were 0.3° in width, and the initial 50 frames were recollected at the end to check for crystal degradation — none was noted. Cell refinements and data reductions were carried out with SAINT in APEX2 [16]. Straightforward determinations of the structure were carried out by direct methods with XS and refinement with XL of the SHELX [17] package. Displacement parameters were refined anisotropically. Numerical face-indexed absorption corrections were applied using SADABS [18]. Secondary corrections for extinction were applied. The crystals from both preparations yielded identical structures, with only small differences in the refinement parameters. Therefore, the structure as solved from the first crystal, which was larger and yielded a better refinement, is presented here. The largest residual electron density is 2.1(3) e Å^{-3}, 0.87 Å away from atom U3. The deepest hole is −1.2(3) e Å^{-3}, 0.42 Å away from atom Se1. The atom positions were standardized using STRUCTURE TIDY [19] in PLATON [20]. Crystallographic details are given in Table 1, and selected metrical details in Table 2. Additional information is in the Supporting material.

Table 1
Crystallographic details for $Cs_3U_{18}Se_{38}$.

Formula mass (g mol^{-1})	7683.75
Space group	D_{4h}^{18}-*I*4/*mcm*
a (Å)	15.3325(3)
c (Å)	26.7223(6)
V (Å^3)	6282.0(2)
ρ_{calc} (g cm^{-3})	8.124
Z	4
T (K)	99(2)
μ(mm^{-1})	69.947
$R(F)$[a]	0.0197
$R_w(F_o^2)$[b]	0.0415

[a] $R(F)=\sum||F_o|-|F_c||/\sum|F_o|$ for $F_o^2>2\sigma(F_o^2)$.

[b] $R_w(F_o^2)=\{\sum w(F_o^2-F_c^2)^2/\sum wF_o^4\}^{1/2}$ For $F_o^2<0$, $w^{-1}=\sigma^2(F_o^2)$; for $F_o^2\geq 0$, $w^{-1}=\sigma^2(F_o^2)+(0.0138F_o^2)^2$.

Table 2
Selected interatomic distances (Å) for $Cs_3U_{18}Se_{38}$.[a]

U1–Se1	2.8111(6)	U3–Se2 (*x*2)	2.9934(5)
U1–Se2	2.8368(6)	U3–Se4 (*x*2)	3.0963(3)
U1–Se1	2.8461(6)	U4–Se5 (*x*2)	2.7687(8)
U1–Se3	2.8566(6)	U4–Se1 (*x*4)	2.8729(6)
U1–Se5	2.9010(4)	U4–Se6 (*x*2)	3.0244(7)
U1–Se6	2.9475(2)	Cs1–Se3 (*x*4)	3.6344(7)
U1–Se7	3.0047(3)	Cs1–Se6 (*x*2)	3.6912(8)
U1–Se2	3.5774(6)	Cs1–Se5 (*x*4)	4.1011(8)
U2–Se4	2.8886(8)	Cs2–Se3 (*x*8)	3.6588(5)
U2–Se6	2.9437(8)	Cs2–Se4 (*x*4)	3.7556(8)
U2–Se3 (*x*2)	2.9902(6)	Se1···Se5	3.3167(9)
U2–Se2 (*x*2)	3.0178(6)	Se3···Se3	3.317(1)
U2–Se4	3.0682(8)	Se1···Se6	3.3230(9)
U2–Se1 (*x*2)	3.0967(6)	Se3···Se6	3.3558(8)
U3–Se3 (*x*2)	2.7976(6)	Se2···Se2	3.412(1)
U3–Se2 (*x*2)	2.9692(6)	Se1···Se1	3.426(1)

[a] High-symmetry sites are: U2 ..*m*; U3. 2.; U4 *m*.2*m*; Cs1 2.*mm*; Cs2 $\bar{4}$2*m*; Se4 ..*m*; Se5 *m*..; Se6 ..*m*; Se7 4..

2.3. Electrical resistivity

A tapered rectangular rod was selected for single-crystal electrical resistivity measurements. The tips were cut off with a razor leaving a rectangular rod with dimensions 0.0323(1) cm × 0.0066(1) cm × 0.0032(1) cm. The long dimension corresponds to the [0 0 1] direction in the structure. Measurements in any other direction were not possible, given the habit of the crystal. Two leads constructed of 8 μm diameter graphite fibers glued to 15 μm diameter copper wires were glued to the ends of the crystal with Dow 4929N silver paint diluted with 2-butoxyethyl acetate. The copper ends of the leads were glued to a TO-8 header, which was in turn soldered onto a Quantum Design resistivity puck (Part 4084-109). Standard two-probe measurements were conducted with a Quantum Design PPMS from 300 K to 25 K, below which the resistivity of the sample exceeded the limits of the instrument.

3. Discussion

3.1. Synthesis

The synthesis of $Cs_3U_{18}Se_{38}$ has proved to be challenging. Attempts at rational syntheses using stoichiometric quantities of U, Se, and Cs_2Se_3 generally failed to produce the desired compound and instead afforded the stable β-USe_2 and CsU_2Se_6 compounds. The U:Se ratio is close to 1:2 in the desired compound vs. 1:3 in CsU_2Se_6, and a starting ratio of 1:2 produced $Cs_3U_{18}Se_{38}$, whereas a 1:3 ratio always failed. Reactions utilizing a CsCl flux also benefitted from less Se.

Inclusion of P or As in the reaction afforded greater quantities of $Cs_3U_{18}Se_{38}$. These elements are likely forming P_2Se_5 or As_2Se_3 in situ. Pnicogen chalcogenides have been used to synthesize other uranium chalcogenides, such as LaU_2Se_9 [21]. Attempts at using Sb or Sb_2Se_3 failed, however, suggesting the size of the pnicogen element plays a role in the crystallization of $Cs_3U_{18}Se_{38}$. Although using UP_2 or As in the reaction encouraged crystal growth, using As_2Se_3 failed to generate crystals of $Cs_3U_{18}Se_{38}$. There clearly are intriguing questions about the mechanism by which crystals of $Cs_3U_{18}Se_{38}$ grow.

3.2. Structure

$Cs_3U_{18}Se_{38}$ crystallizes in a new structure type, in the tetragonal space group *I*4/*mcm* (Fig. 1). The asymmetric unit contains

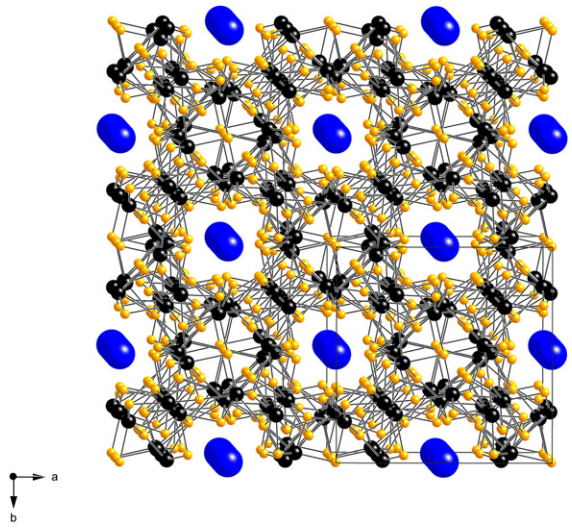

Fig. 1. The structure of $Cs_3U_{18}Se_{38}$ viewed down the *c* axis. Cs atoms are blue, U atoms are black, and Se atoms are yellow. Cs–Se bonds are omitted. (For interpretation of the references to colour in this figure legend, the reader is referred to the web version of this article.)

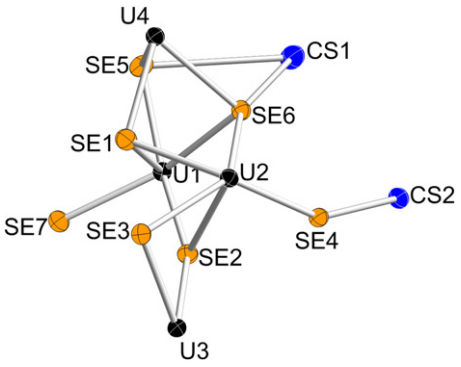

Fig. 2. Asymmetric unit of $Cs_3U_{18}Se_{38}$. Displacement ellipsoids are drawn at the 95% probability level.

two crystallographically independent Cs atoms, four such U atoms, and seven such Se atoms (Fig. 2). Atom U1 is coordinated by seven Se atoms in an augmented triangular prismatic geometry (Fig. 3(a)) that is also found in $UY_4O_3S_5$ where it is referred to as a seven-octahedron [22]. Atom U2 (site symmetry ..*m*) is in a monocapped square antiprism (Fig. 3(b)), which is also found in $La_2U_2Se_9$ [21]. Atom U3 (site symmetry .2.) is in a distorted square antiprism (Fig. 3(c)), and atom U4 (site symmetry *m*.2*m*) is in a bicapped trigonal prism (Fig. 3(d)). This coordination is found in the AAn_2Q_6 compounds [4], and can be considered a slight distortion of a triangulated dodecahedron, found in the compounds MU_8Q_{17} (M=transition metal) [23,24].

The overall structure contains channels along the *c* axis, with the network around them composed of USe_x coordination polyhedra. The complex structure may most easily be described by dividing it into two kinds of chains along [0 0 1]. The first chain is composed of U1 and U3 polyhedra. A $U1Se_7$ polyhedron edge shares with a $U3Se_8$ polyhedron along one of the edges on the axial "crown." Another $U1Se_7$ polyhedron edge shares on the opposite edge of the first $U1Se_7$ polyhedron. These units corner share such that there are six of these U polyhedra in one chain in a unit cell. The pattern is ...U1–U3–U1–U1–U3–U1... Three more of these chains are generated by symmetry. Four of the $U1Se_7$ polyhedra are situated around a single shared Se atom, which sits on a four-fold rotation center. Each of these polyhedra edge shares with the two neighboring polyhedra. The four $U3Se_8$ polyhedra edge share along opposite edges of one square face (Fig. 4).

The second chain comprises $U2Se_9$ and $U4Se_8$ polyhedra. A $U4Se_8$ polyhedron face shares on both of the triangular trigonal prism faces with $U2Se_9$ polyhedra along the trigonal crown faces. The $U2Se_9$ polyhedra edge share, where one of the shared vertices is the capping Se atom (Fig. 5). The overall pattern for this chain is ...U4–U2–U2–U4–U2–U2... The two kinds of chains are staggered, and the U2–U4 chain undulates such that when the U2 polyhedron face shares with a U1 polyhedron, it edge shares with the other closest U1 polyhedron. U2 polyhedra edge share with U3 polyhedra, and U4 polyhedra face and corner share with U1 polyhedra (Fig. 6). The overall structure comprises four of the U1–U3 chains in the center of the cell and one on each corner,

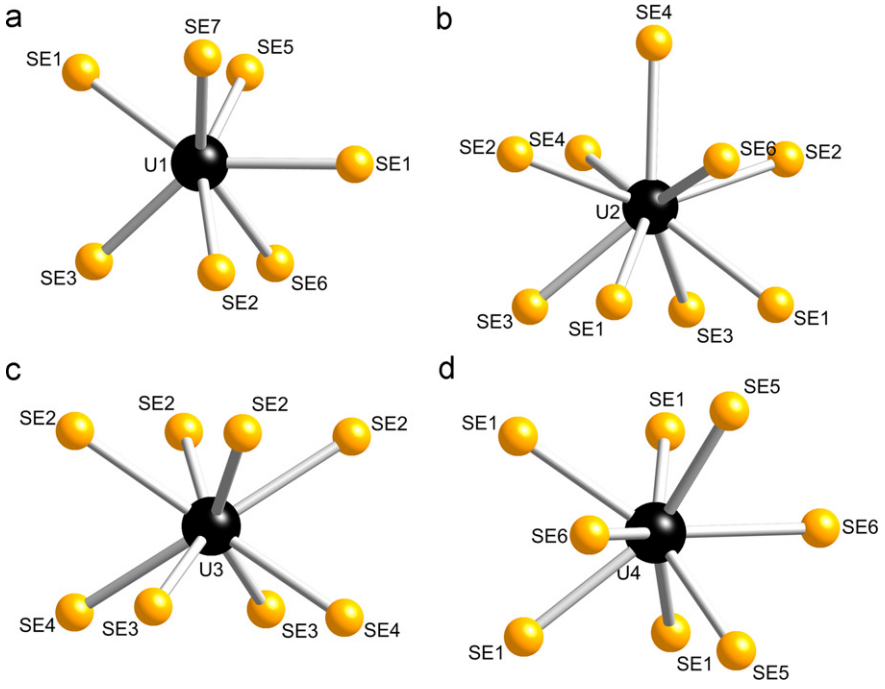

Fig. 3. Coordination environments of atoms U1 (a), U2 (b), U3 (c), and U4 (d).

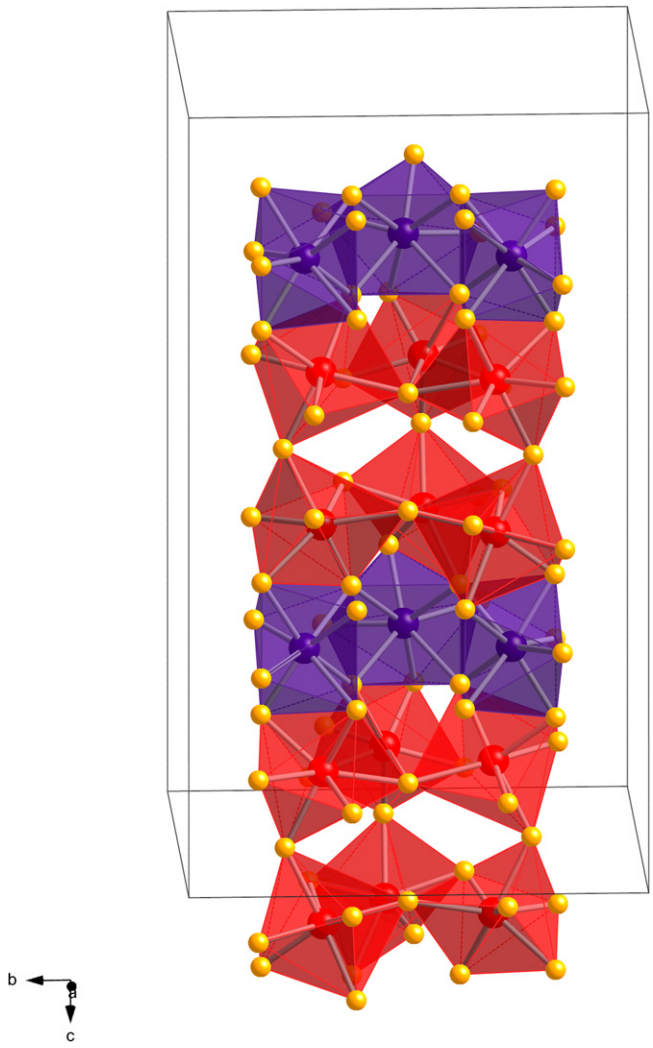

Fig. 4. Connectivity of the U1–U3 chains. U1 and U3 polyhedra are red and purple, respectively. One chain is omitted. (For interpretation of the references to colour in this figure legend, the reader is referred to the web version of this article.)

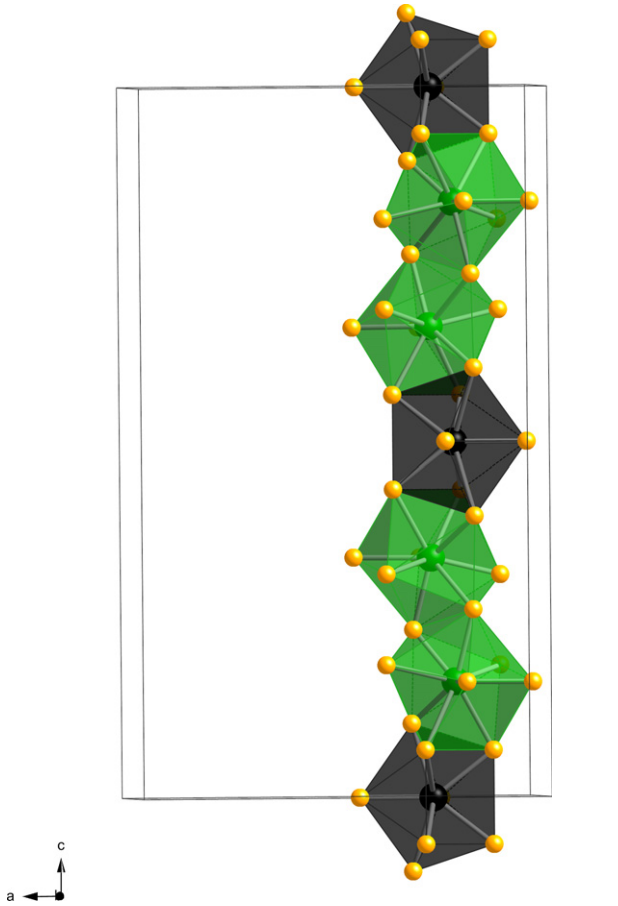

Fig. 5. Connectivity of a U2–U4 chain. U2 and U4 polyhedra are green and black, respectively. (For interpretation of the references to colour in this figure legend, the reader is referred to the web version of this article.)

which corner share at one vertex of the U1 polyhedron with another group of four chains. These chains are further connected by one U2–U4 chain. Four U1–U3 chains sit in the center of the unit cell, one at each corner, and Cs atoms sit on the edges of the unit cell (Fig. 7).

Interatomic distances are typical. U1–Se distances range from 2.8111(6) Å to 3.0047(3) Å, with an additional long distance of 3.5774(6) Å. Compare these to 2.906 Å to 3.043 Å, with an additional distance of 3.628 Å in U_2Se_3 [25]. U2–Se distances are in the range of 2.8886(8) Å to 3.0967(6) Å, comparable to 2.818(6) Å to 3.123(4) Å in γ-USe_2 [26]. U3–Se distances are in the range of 2.7967(6) Å to 3.0963(3) Å, and U4–Se distances are in the range of 2.7687(8) Å to 3.0244(7) Å. Compare these to that for eight-coordinate U in $CoUSe_{2.7}$ of 2.628 Å to 3.104 Å [27]. Among these comparisons only in γ-USe_2 is the U clearly tetravalent.

The following compounds have these shortest Se⋯Se distances: $Cs_2Pd_3USe_6$—3.334(1) Å [28]; $PdUSe_3$ — 3.375(2) Å [29]; PbU_2Se_5—3.334 Å [30]. These Se⋯Se distances are very long compared to a Se–Se single-bond distance of 2.33 Å. These compounds charge balance with formal charges of Cs^+, Pd^{2+}, U^{4+}, Pb^{2+}, and Se^{2-} For comparison, the shortest Se⋯Se distance in $Cs_3U_{18}Se_{38}$ is 3.3167(9) Å (Table 2). Thus, Se–Se bonding interactions may also be ruled out in $Cs_3U_{18}Se_{38}$.

3.3. Formal oxidation states

If we assign the formal oxidation states Cs^+, U^{4+}, and Se^{2-}, then the net charge in $Cs_3U_{18}Se_{38}$ is $3\times1+18\times4-38\times2=-1$. Possible reasons for this charge imbalance are (1) inclusion of an impurity in the structure, (2) Se deficiency, or (3) mixed oxidation states for U. None of these can be assessed from the crystal structure refinements.

The same structure results when synthesized with or without Ni and CsCl. Therefore, the possible impurities are limited to P^{5+} or As^{5+} substituting for U^{4+}. The required atomic percentage for any such impurity would be 1.7%, as one out of every 59 atoms would have to be substituted. Such quantities should have been detectable by EDS. Another possibility is Se atom deficiency to the extent that the actual formula is $Cs_3U_{18}Se_{37.5}$. The fact that the weight percent of Se decreases only slightly from 39.05% to 38.74% for the formula $Cs_3U_{18}Se_{38}$ to $Cs_3U_{18}Se_{37.5}$ makes a chemical analysis infeasible, even if sufficient material were available.

The remaining possibility is the presence of U^{5+} in the structure, so that the formula may be written $Cs_3^+U^{5+}U_{17}^{4+}Se_{38}^{2-}$. A number of compounds have been reported where U has been assigned the mixed U^{4+}/U^{5+} oxidation states, including $Pd_3U_{0.92}S_4$ [31], $Cu_2U_3S_7$ [32], and Mo_6US_8 [33]. The refinement of the present single-crystal X-ray data is insensitive to the presence of $1U^{5+}$: $17U^{4+}$ in the asymmetric unit.

3.4. Electrical resistivity

The temperature dependence of the resistivity, ρ, in the [0 0 1] direction of a single crystal is presented in Fig. 8. $Cs_3U_{18}Se_{38}$

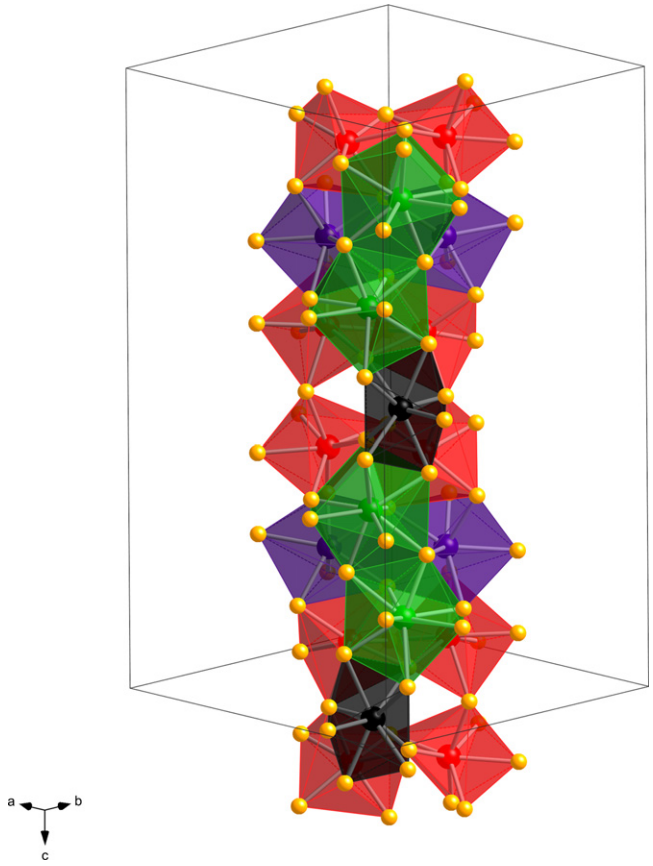

Fig. 6. Connectivity of two U1–U3 chains with a U2–U4 chain.

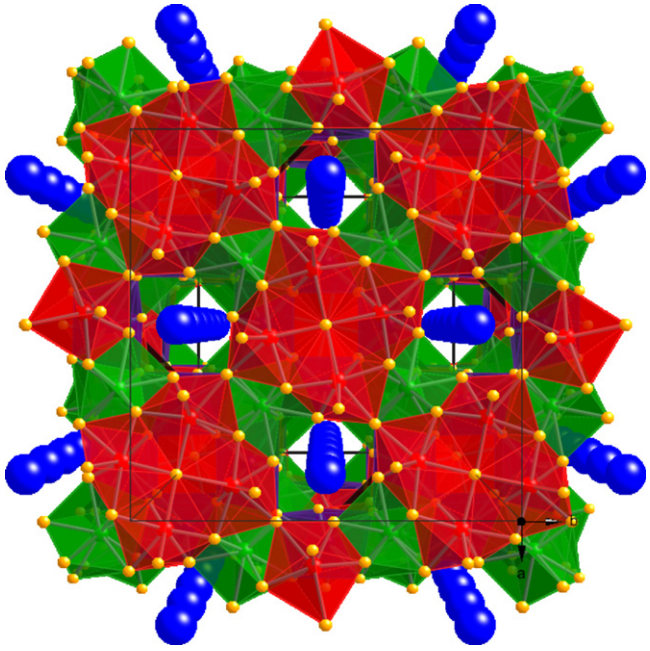

Fig. 7. Overall structure of $Cs_3U_{18}Se_{38}$, with the chains colored differently. (For interpretation of the references to colour in this figure legend, the reader is referred to the web version of this article.)

displays typical semiconductor behavior from 57 to 225 K ($0.018\ K^{-1}$ to $0.0044\ K^{-1}$). The resistivity plot was fit to the Arrhenius thermal energy equation $\rho=\rho_0 \exp(E_a/k_BT)$ by plotting $\ln(\rho)$ versus T^{-1}, where E_a is the activation energy (Fig. 9). The slope of the linear portion of the plot, E_a/k_B, is related to the band

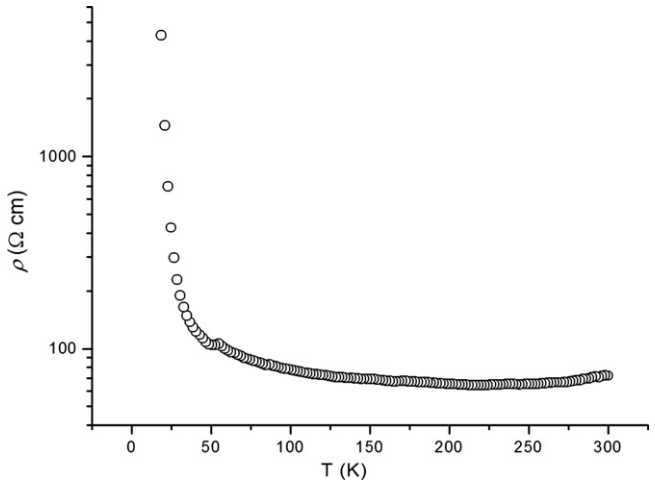

Fig. 8. Electrical resistivity versus temperature for $Cs_3U_{18}Se_{38}$.

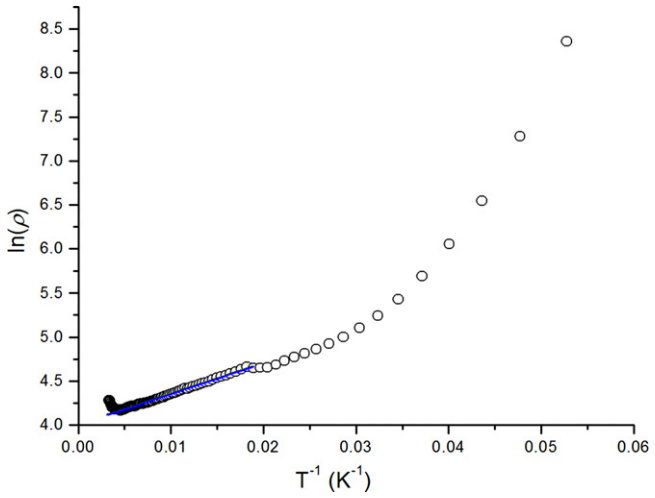

Fig. 9. Plot of natural logarithm of resistivity versus inverse temperature. The linear portion of the curve is marked with a blue line. (For interpretation of the references to colour in this figure legend, the reader is referred to the web version of this article.)

gap by the expression $E_g=2E_a$. A fit to the linear portion of the data results in $E_a=0.0030(1)$ eV. The resistivity of $Cs_3U_{18}Se_{38}$ at 300 K is 72 Ω cm. The resistivity and calculated band gap are significantly lower than those of KU_2Se_6 ($\rho_{300}=1000\ \Omega$ cm; $E_a=0.27$ eV) [6] and RbU_2Se_6 ($\rho_{300}=1.7\times10^4\ \Omega$ cm; $E_a=0.159(1)$ eV). [4] They are, however, larger than those of Na_2US_3 ($\rho_{300}=1.14\ \Omega$ cm; $E_a=0.001$–0.002 eV) [34].

Between 25 K and 57 K, the curve follows more unusual semiconductor behavior (Fig. 9). Below 25 K the resistivity of the sample exceeds the limits of the instrument. Above 225 K the resistivity increases with increasing temperature. Whereas the two-point probe method does include the resistivity of the leads, the resistivity at room temperature of Cu is $1.68^{-6}\ \Omega$ cm, well below the minimum observed resistivity of 64 Ω cm. Graphite similarly has a low resistivity of up to 0.30 Ω cm, and as a semiconductor its effect on the curve is to make the high-temperature part less prominent. This feature in the curve is thus intrinsic to the compound. This change in slope is inconsistent with semiconductor behavior, and may indicate a metal-to-insulator transition. Such transitions are typically more dramatic such as in NiS_ySe_{1-y} [35], but compounds such as $La_{1-x}Sr_xTiO_3$ display such broad transitions [36].

4. Final remarks

$Cs_3U_{18}Se_{38}$ crystallizes in a new structure type, which contains Cs atoms in channels formed by a network of U and Se atoms. The structure contains U coordinated in four distinct coordination environments, which are fairly typical of those found in A/U/Q compounds. This compound cannot be charge balanced by assigning whole-number formal oxidation states to the elements. Possible rationalizations include a Se atom deficiency or a mixed U^{4+}/U^{5+} oxidation state. Single-crystal electrical resistivity measurements show the presence of a possible metal-to-insulator transition at 225 K, atypical semiconductor behavior below 57 K, and an activation energy of 0.0030(1) eV, smaller than that of RbU_2Se_6, but larger than that of Na_2US_3.

Supporting information

The crystallographic data for $Cs_3U_{18}Se_{38}$ have been deposited with FIZ Karlsruhe as CSD number 423658. These data may be obtained free of charge by contacting FIZ Karlsruhe at +497247808666 (fax) or crysdata@fiz-karlsruhe.de (email).

Acknowledgments

The work presented was supported by the U.S. Department of Energy, Basic Energy Sciences, Chemical Sciences, Biosciences, and Geosciences Division and Division of Materials Science and Engineering Grant ER–15522. SEM analyses were conducted in the Electron Probe Instrumentation Center (EPIC) at the Northwestern University Atomic and Nanoscale Characterization Experimental (NUANCE) Center, supported by NSF-NSEC, NSF-MRSEC, Keck Foundation, the State of Illinois, and Northwestern University. Crystallographic data were collected at the IMSERC X-ray Facility at Northwestern University, supported by the International Institute of Nanotechnology (IIN). Use was made of the Magnet and Low Temperature facility operated by the NSF-supported Northwestern University Materials Research Center.

Appendix A. Supplementary material

Supplementary data associated with this article can be found in the online version at http://dx.doi.org/10.1016/j.jssc.2012.02.035.

References

[1] H. Masuda, T. Fujino, N. Sato, K. Yamada, M. Wakeshima, J. Alloys Compd. 284 (1999) 117–123.
[2] K. Stöwe, S. Appel-Colbus, Z. Anorg. Allg. Chem. 625 (1999) 1647–1651.
[3] J. Padiou, J. Lucas, C.R. Acad., Sci. Ser. IIc: Chim. 263 (1966) 71–73.
[4] D.E. Bugaris, D.M. Wells, J. Yao, S. Skanthakumar, R.G. Haire, L. Soderholm, J.A. Ibers, Inorg. Chem. 49 (2010) 8381–8388.
[5] E.J. Wu, M.A. Pell, J.A. Ibers, J. Alloys Compd. 255 (1997) 106–109.
[6] H. Mizoguchi, D. Gray, F.Q. Huang, J.A. Ibers, Inorg. Chem. 45 (2006) 3307–3311.
[7] B.C. Chan, Z. Hulvey, K.D. Abney, P.K. Dorhout, Inorg. Chem. 43 (2004) 2453–2455.
[8] K.-S. Choi, R. Patschke, S.J.L. Billinge, M.J. Waner, M. Dantus, M.G. Kanatzidis, J. Am. Chem. Soc. 120 (1998) 10706–10714.
[9] J.A. Cody, J.A. Ibers, Inorg. Chem. 35 (1996) 3836–3838.
[10] J.A. Cody, J.A. Ibers, Inorg. Chem. 34 (1995) 3165–3172.
[11] A.C. Sutorik, M.G. Kanatzidis, J. Am. Chem. Soc. 113 (1991) 7754–7755.
[12] D.E. Bugaris, J.A. Ibers, J. Solid State Chem. 181 (2008) 3189–3193.
[13] A.J.K. Haneveld, F. Jellinek, J. Less-Common Met. 18 (1969) 123–129.
[14] S.A. Sunshine, D. Kang, J.A. Ibers, Mater. Res. Soc. Symp. Proc. 97 (1987) 391–396.
[15] H. Noël, M. Potel, R. Troc, L. Shlyk, J. Solid State Chem. 126 (1996) 22–26.
[16] Bruker, APEX2 version 2009.5-1 and SAINT version 7.34a data collection and Processing Software, 2009. Bruker Analytical X-Ray Instruments, Inc.: Madison, WI, USA.
[17] G.M. Sheldrick, Acta Crystallogr., Sect. A: Found. Crystallogr. 64 (2008) 112–122.
[18] G.M. Sheldrick, SADABS, Department of Structural Chemistry, University of Göttingen, Göttingen, Germany, 2008.
[19] L.M. Gelato, E. Parthé, J. Appl. Crystallogr. 20 (1987) 139–143.
[20] A.L. Spek, PLATON, A multipurpose crystallographic tool, 2008. Utrecht University, Utrecht, The Netherlands.
[21] D.E. Bugaris, R. Copping, T. Tyliszczak, D.K. Shuh, J.A. Ibers, Inorg. Chem. 49 (2010) 2568–2575.
[22] G.B. Jin, E.S. Choi, D.M. Wells, J.A. Ibers, J. Solid State Chem. 182 (2009) 1861–1866.
[23] H. Noël, M. Potel, J. Padiou, Acta Crystallogr., Sect B. Struct. Crystallogr., Cryst. Chem. 31 (1975) 2634–2637.
[24] H. Noël, C.R. Seances, Acad. Sci., Ser. C 277 (1973) 463–464.
[25] P. Khodadad, C.R. Hebd. Seances Acad. Sci. 249 (1959) 694–696.
[26] H. Kohlmann, H.P. Beck, Z. Anorg. Allg. Chem. 623 (1997) 785–790.
[27] H. Noël, C.R. Seances Acad. Sci. Ser. C 279 (1974) 513–515.
[28] G.N. Oh, J.A. Ibers, Acta Crystallogr. E67 (2011) i9.
[29] A. Daoudi, H. Noël, J. Less-Common Met. 153 (1989) 293–298.
[30] M. Potel, R. Brochu, J. Padiou, Mater. Res. Bull. 10 (1975) 205–208.
[31] A. Daoudi, H. Noël, Inorg. Chim. Acta 117 (1986) 183–185.
[32] A. Daoudi, M. Lamire, J.C. Levet, H. Noël, J. Solid State Chem. 123 (1996) 331–336.
[33] A. Daoudi, M. Potel, H. Noël, J. Alloys Compd. 232 (1996) 180–185.
[34] H. Masuda, T. Fujino, N. Sato, K. Yamada, Mater. Res. Bull. 34 (1999) 1291–1300.
[35] S. Anzai, M. Matoba, M. Hatori, H. Sakamoto, J. Phys. Soc. Jpn. 55 (1986) 2531–2534.
[36] T. Katsufuji, Y. Tokura, Phys. Rev. B 50 (1994) 2704–2707.